AIAA JOURNAL
Vol. 39, No. 10, October 2001

Three-Dimensional Analytic Model of Vibrational Energy Transfer in Molecule–Molecule Collisions

Igor V. Adamovich*
The Ohio State University, Columbus, Ohio 43210-1107

A three-dimensional semiclassical analytic model of vibrational energy transfer in collisions between two rotating diatomic molecules has been extended for molecule–molecule collision. The model is based on analysis of classical trajectories of free-rotating (FR) molecules acted upon by a superposition of repulsive exponential atom-to-atom potentials. The energy transfer probabilities have been evaluated using the nonperturbative Forced Harmonic Oscillator (FHO) model. The model predicts the probabilities for vibrational energy transfer as functions of the total collision energy, orientation of molecules during a collision, their rotational energies, and impact parameter. The model predictions have been compared with the results of three-dimensional close-coupled semiclassical trajectory calculations using the same potential energy surface. The comparison demonstrates not only remarkably good agreement between the analytic and numerical probabilities across a wide range of collision energies, but also shows that the analytic FHO-FR model correctly reproduces the probability dependence on other collision parameters such as rotation angles, angular momentum angles, rotational energies, and impact parameter. The model equally well predicts the cross sections of single-quantum and multiquantum transitions and is applicable up to very high collision energies and quantum numbers. Most importantly, the resultant analytic expressions for the probabilities do not contain any arbitrary adjustable parameters commonly referred to as *steric factors*. The present work essentially completes development of the analytic rate database for vibrational energy transfer among air species, increasing the range of applicability of the FHO-FR model.

I. Introduction

VIBRATIONAL energy transfer processes in collisions of diatomic molecules play an extremely important role in gas discharges, molecular lasers, plasma chemical reactors, high-enthalpy gas dynamic flows, and in the physics of the upper atmosphere. In these nonequilibrium environments the energy loading per molecule can be as high as 0.1–5.0 eV, whereas disequipartition among translational, vibrational, and electronic energy modes of heavy species, and with the free electron energy, can be very strong. This often results in development and maintaining of strongly nonequilibrium molecular vibrational energy distributions, which induce a variety of energy transfer processes among different energy modes and species, chemical reactions, and ionization.[1–3] The rates of these processes are determined by the populations of high vibrational levels of molecules, which are often controlled by vibration-vibration-translation (V-V-T) processes

$$\mathrm{AB}(i_1) + \mathrm{CD}(i_2) \rightarrow \mathrm{AB}(f_1) + \mathrm{CD}(f_2) \qquad (1)$$

In Eq. (1) AB and CD represent diatomic molecules and an atom, respectively, and i_1, i_2, f_1, and f_2 are vibrational quantum numbers. Traditionally, these processes are separated into two separate modes: 1) vibration-translation (V-T) processes [$i_2 = f_2$ in Eq. (1)] and 2) vibration-vibration (V-V) processes [$i_1 - f_1 = f_2 - i_2$ in Eq. (1)]. At the low temperatures the V-T processes are typically much slower than V-V energy transfer.

Quantitative data on the mechanisms and kinetic rates of these processes are needed for numerous practical applications, including novel chemical technologies, environmental pollution control, and radiation prediction in aerospace propulsion flows, in high-altitude rocket plumes and behind shock waves. In addition, recent results demonstrate that strong vibrational disequilibrium can be sustained in CO-seeded atmospheric pressure air, optically pumped by a low-power c.w. CO laser.[4] This opens a possibility of creating stable large-volume high-pressure air plasmas. Insight into kinetics of these plasmas also requires knowledge of V-T and V-V rates in CO, N_2, and O_2.

Received 25 July 2000; revision received 1 February 2001; accepted for publication 1 March 2001.

*Visiting Assistant Professor, Nonequilibrium Thermodynamics Laboratory, Department of Mechanical Engineering. Senior Member AIAA.

There exists an extensive literature on the experimental study of V-T and V-V energy transfer, including recent state-specific rate measurements for highly vibrationally excited molecules, such as NO, O_2, and CO (Refs. 5–9). However, for many energy transfer processes among high vibrational quantum numbers the experimental rate data are still unavailable. As a result, most such rates used in applied kinetic modeling are based on theoretical scattering calculations. Among numerous theoretical rate models available, one can separate the following major approaches: 1) fully quantum calculations; 2) classical, quasiclassical, and semiclassical numerical trajectory calculations; and 3) analytic methods.

Because the exact quantum calculations are rather computationally laborious, they have been usually made for a simplified model of collinear collisions of harmonic oscillators and used as tests for more approximate approaches.[10–12] However, some three-dimensional calculations of the state-specific vibrational energy transfer rates for O_2–O_2 using vibrational close-coupling infinite-order sudden approximation have been recently published.[13]

Classical and quasiclassical trajectory methods, such as used for calculations of vibrational relaxation rates for O_2–Ar (Ref. 14), N_2–N, and O_2–O (Refs. 15 and 16), are applicable only for calculation of rather large transition probabilities. For accurate predictions of small transition probabilities $P \ll 1$, a large number of collision trajectories $N \sim 1/P$ have to be averaged.

Among semiclassical calculations, one can mention the close-coupled method developed by Billing and validated by comparison with the exact quantum calculations, as well as with experimental data.[17] Trajectory calculations by this method have been made for a number of species such as H_2, N_2, O_2, and CO (Refs. 18–23) in a wide range of collision energies and vibrational quantum numbers. These results comprise perhaps the most extensive and consistent vibrational energy transfer rate database.

In addition to some fundamental problems encountered in calculations by these advanced methods (such as the choice of the three-dimensional potential energy surface), their results are often difficult to interpret and use in kinetic modeling calculations. First, it is not always possible to identify the key energy transfer mechanisms that control the cross sections obtained. Second, the number of the state-specific rates used as entries in modern master equation kinetic models for studies of strongly nonequilibrium gases and plasmas can reach 10^4–10^5. Even if some of these rate data are available from three-dimensional computer calculations, one has to

rely on curve-fitting, unreliable extrapolation, or inaccurate analytic parametrization to incorporate the rates into the model. As a result, such kinetic models do not provide new insight into kinetics, have limited applicability, and lack predictive capability.

Approximate analytic rate expressions are also widely used in kinetic modeling, mostly because of their simplicity. However, available analytic models have serious inherent flaws that make them much less reliable and accurate compared to numerical scattering calculations. First, most of these models, such as the Schwartz, Slawsky, Herzfeld (SSH) theory, Rapp–Englander–Golden model, Sharma–Brau theory, etc.,[24–27] are based on first-order perturbation theory and therefore cannot be applied at high collision energies, high quantum numbers, and for multiquantum processes [$|i-f|>1$ in Eqs. (1) and (2)]. An exception is the nonperturbative Forced Harmonic Oscillator (FHO) model,[28–31] which takes into account the coupling of many vibrational states during a collision, and is therefore applicable for such conditions. Second, analytic models are typically developed only for collinear collisions of nonrotating molecules. A procedure commonly used to account for the effects of realistic three-dimensional collisions and molecular rotation is the introduction of adjustable correction parameters ("steric factors") into the resultant rate expression.[32] These coefficients, which are assumed to be temperature independent, have very little or no theoretical basis and are found from comparison of a simple model with experiments or three-dimensional calculations.

There have been various attempts to develop nonempirical expressions for the steric factors and also to incorporate the effect of rotation into analytic models.[32–35] In most of them, the simplifying assumptions made, such as analyzing of collisions of arbitrarily oriented, but nonrotating, molecules,[32] or, on the contrary, considering only collisions of rapidly rotating "breathing spheres" (i.e., isotropic three-dimensional oscillators),[33–35] were unrealistic. In addition, the coupled effects of orientation of colliding partners, molecular rotation, and nonzero impact parameter collisions have been analyzed separately. Finally, the procedure of comparison between the experimental relaxation rates and the analytic rates corrected for noncollinear orientation and rotation, used by some authors to validate theoretically obtained values of the steric factors, is hardly conclusive. In such cases the agreement obtained might well be caused by the formal adjustment of the intermolecular potential parameters used, i.e., to a curve fitting. The only credible procedure for analytic model validation would be comparing its predictions with the results of three-dimensional numerical calculations made for the same potential energy surface.

The present paper discusses further development of a semiclassical analytic vibrational relaxation model that incorporates the effects of three-dimensional collisions and molecular rotation [Forced Harmonic Oscillator–Free Rotator (FHO-FR) model.[36,37]] It is a follow up on our previous publication,[37] where we analyzed energy transfer in collisions between a diatomic molecule and an atom. Previous results demonstrated not only remarkably good agreement between the analytic and numerical probabilities across a wide range of collision energies, but also showed that the analytic FHO-FR model correctly reproduces the probability dependence on other collision parameters such as rotation angle, angular momentum angle, rotational energy, impact parameter, and collision reduced mass. The model equally well predicted the cross sections of single-quantum and multiquantum transitions up to very high collision energies and quantum numbers.

The main goal of the present study is development of analytic transition probabilities that are in agreement with trajectory calculations and that can be easily incorporated in nonequilibrium kinetic models. Such a model would give new insight into mechanisms of vibrational relaxation, as well as bridge the gap between state-of-the-art theoretical scattering techniques and their use for practical applications.

II. Collision Trajectories and Transition Probabilities

The analysis of the dynamics of collisions between two rotating symmetric diatomic molecules is a straightforward extension of the procedure used for atom-molecule collisions in Ref. 37. The translational motion and the three-dimensional rotation of the molecules

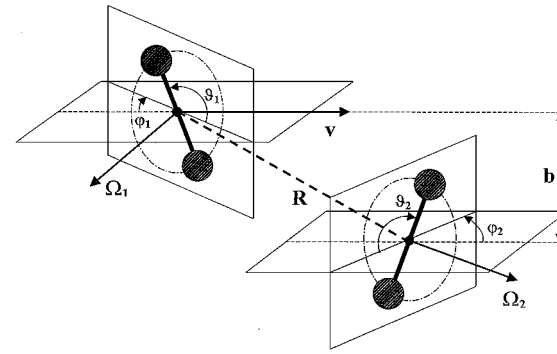

Fig. 1 Schematic of the collision geometry.

are assumed to be uncoupled, and the latter is unaffected by the collision, i.e., free. Then the only effect of rotation on the collision trajectory is the periodic modulation of the interaction potential. The assumption of free rotation is quite similar to the basic assumption made in all semiclassical theories, which evaluate the translational-rotational trajectory uncoupled from the vibrational motion of the oscillator. Also, instead of relying on perturbation theory, the exact semiclassical solution of the Schrodinger equation (the FHO theory[28–31]) is used to evaluate the vibrational transition probabilities. This expands the applicability of the model to high collision energies and allows prediction of multiquantum vibrational transition rates.

Consider a three-dimensional collision of two symmetric molecules (Fig. 1). For the pairwise atom-to-atom interaction described by a repulsive exponential function $U_i(R_i)=A\exp(-\alpha R_i)$, where R_i is the distance between the atoms, the atom-molecule interaction potential can be written as follows:

$$U(R,r,\vartheta_1,\varphi_1,\vartheta_2,\varphi_2)=4Ae^{-\alpha R}\cosh[(\alpha r/2)\cos\vartheta_1\cos\varphi_1]\times\cosh[(\alpha r/2)\cos\vartheta_2\cos\varphi_2] \quad (2)$$

In Eq. (2) R is the center-of-mass distance, r is the separation of atoms in a molecule, ϑ_1 and ϑ_2 are the rotation angles, and φ_1 and φ_2 are the angles between the plane of rotation and the velocity vector $\boldsymbol{v}$ (Fig. 1). Because the rotation is assumed to be free, neither the magnitude nor the direction of the angular momentum vectors change in a collision. That gives $\vartheta_i(t)=\vartheta_{i0}+\Omega_i t$, $\varphi_i(t)=\varphi_{i0}$, where Ω_i are the constant angular velocities of molecular rotation and the subscript 0 means "at the point of maximum interaction," where U is maximum. To calculate the semiclassical trajectory $R(t)$, we also assume $r(t)=r_e$, where r_e is the equilibrium atom separation. One can see that the potential (2) consists of the exponential translational part modulated by the periodic rotational factors. If the rotation is not very rapid, the modulation can substantially change the shape of the time-dependent perturbation $U(\tilde{R},t)$, where $\tilde{R}(t)=R(t)-R_0$ and R_0 is the "collision diameter" (the distance at the maximum interaction point). The classical equation of motion for this potential $m\ddot{\tilde{R}}(t)=-\partial U(\tilde{R},t)/\partial\tilde{R}$ (m is the collision reduced mass) can be easily solved if the rotation is slow, so that the potential $U(R,r_e,t)=U(\tilde{R},t)$ can be expanded near the point of maximum interaction R_0.

This approach also allows incorporation of nonzero impact parameter collisions by taking into account only radial relative motion of the colliding partners $R(t)$ in the vicinity of the maximum interaction point. Then the translational energy of collision $E_{\rm tr}=E-E_{\rm rot,1}-E_{\rm rot,2}$ is replaced by the energy of the radial motion $E_{\rm rad}=(E-E_{\rm rot,1}-E_{\rm rot,2})[1-b^2/R(t)^2]\cong(E-E_{\rm rot,1}-E_{\rm rot,2})(1-b^2/R_0^2)$ (the so-called modified wave-number approximation[34]). Here E is the total collision energy, $E_{{\rm rot},i}=m_{0,i}\Omega_i^2 r_e^2/2$ are rotational energies of the molecules, $m_{0,i}$ are the oscillator reduced masses, and b is the impact parameter. This approach is justifiable for short-range repulsive interactions when the energy transfer is determined by a small portion of the trajectory near the maximum interaction point.[38] The resultant expression for the trajectory is

$$U(t) = \frac{E\gamma^2}{\cosh^2[\gamma\alpha t\sqrt{E/2m}]} \tag{3}$$

$$\gamma(\varepsilon, y, \vartheta_{10}, \varphi_{10}, \vartheta_{20}, \varphi_{20}) \approx \max\left[0, -\frac{\sin 2\vartheta_{10}\cos\varphi_{10}}{2}\sqrt{\varepsilon_1} - \frac{\sin 2\vartheta_{20}\cos\varphi_{20}}{2}\sqrt{\varepsilon_2} + \sqrt{(1-\varepsilon_1-\varepsilon_2)(1-y)}\right] \tag{4}$$

Equation (3) describes a parametric set of three-dimensional trajectories with the same total collision energy E and various values of rotational energies, impact parameter, and orientation of collision partners, characterized by a single factor $\gamma = (\varepsilon, y, \vartheta_{10}, \varphi_{10}, \vartheta_{20}, \varphi_{20})$, which is given by Eq. (4). In Eq. (4), $\varepsilon_i = E_{\mathrm{rot},i}/E$, and $y = b^2/R_0^2$. The factor $E\gamma^2$ in Eq. (3) can be interpreted as the effective collision energy. One can see that at $\varepsilon_i = y = \vartheta_{i0} = \varphi_{i0} = 0$ one has $\gamma = 1$, $E = E_{\mathrm{tr}}$, and the trajectory coincides with the one-dimensional result for a head-on collinear collision of two nonrotating molecules.[39]

The applicability of Eqs. (3) and (4) is limited to relatively slow molecular rotation [37] when

$$\varepsilon_1 + \varepsilon_2 = (E_{\mathrm{rot},1} + E_{\mathrm{rot},2})/E \lesssim \frac{1}{2}\frac{(1-y^2)}{(1-y^2/2)} \tag{5}$$

so that the collision trajectory of a rapidly rotating molecule cannot be accurately predicted, especially at large impact parameters. However, the contribution of such collisions to the overall transition probability as a function of the total collision energy E is expected to be small (see discussion in Ref. 37). Therefore, in the present paper we disregard such collisions. Later we will show that this assumption is consistent with the results of the three-dimensional trajectory calculations.

Having calculated the free rotation collision trajectory (3) and (4), we can evaluate the semiclassical vibrational energy transfer probabilities $P(i_1, i_2 \to f_1, f_2)$, where i and f are initial and final vibrational quantum numbers, respectively. For this we will use the FHO theory,[28–31] a nonperturbative analytic model, originally developed for collinear collisions of nonrotating diatomic molecules. This model is based on the exact solution of the Schrodinger equation for the intermolecular potential $U(R, r, \vartheta_i, \varphi_i)$ linearized in r and therefore takes into account the coupling of all vibrational quantum states during a collision. It is applicable up to high collision energies and vibrational quantum numbers, as well as for multiquantum transitions. The scaling law predicted by this model, i.e., the probability dependence on the vibrational quantum numbers, is independent of the interaction potential. Unfortunately, the exact FHO expression for a general V-V-T process probability $P(i_1, i_2 \to f_1, f_2)$ is extremely cumbersome.[30] However, FHO probabilities of the V-T processes $P(i_1, 0 \to f_1, 0)$ and of the V-V process $P(i_1, i_2 \to f_1, f_2)$, $i_1 - f_1 = f_2 - i_2$, are much simpler. They are given by the following relations[37,40,41]:

$$P(i_1, 0 \to f_1, 0) \approx \frac{(n_s)^s}{(s!)^2}Q^s \times \exp\left[-\frac{2n_s}{s+1}Q - \frac{n_s^2}{(s+1)^2(s+2)}Q^2\right]$$

$$s = |i_1 - f_1|, \qquad n_s = \left[\frac{\max(i_1, f_1)!}{\min(i_1, f_1)!}\right]^{1/s} \tag{6}$$

for the V-T processes, and

$$P(i_1, i_2 \to f_1, f_2) \approx \frac{(n_{s,1})^s (n_{s,2})^s}{(s!)^2}G^s \times \exp\left[-\frac{2n_s}{s+1}G - \frac{n_s^2}{(s+1)^2(s+2)}G^2\right]$$

$$s = |i_1 - f_1| = |i_2 - f_2|, \qquad n_{s,1} = \left[\frac{\max(i_1, f_1)!}{\min(i_1, f_1)!}\right]^{1/s} \times n_{s,2} = \left[\frac{\max(i_2, f_2)!}{\min(i_2, f_2)!}\right]^{1/s} \tag{7}$$

for the V-V processes. In Eqs. (6) and (7) the potential-dependent parameters Q and G are the following trajectory integrals[28–30]:

$$Q = \frac{\langle 1|\tilde{r}|0\rangle_1^2}{\hbar^2}\left|\int_{-\infty}^{\infty}\left[\frac{\partial U(\tilde{R}, \tilde{r}, t)}{\partial \tilde{r}}\right]_{\tilde{r}=0} e^{i\omega_1 t}\,\mathrm{d}t\right|^2 \tag{8}$$

$$G = \frac{\langle 1|\tilde{r}|0\rangle_1^2\langle 1|\tilde{r}|0\rangle_2^2}{\hbar^4}\left|\int_{-\infty}^{\infty}\left[\frac{\partial U(\tilde{R}, \tilde{r}, t)}{\partial \tilde{r}}\right]_{\tilde{r}=0} e^{i(\omega_1-\omega_2)t}\,\mathrm{d}t\right|^2 \tag{9}$$

In Eqs. (8) and (9), $\tilde{r} = r - r_e$, $\omega_j = |E_{i_j} - E_{f_j}|/s\hbar$ is the average vibrational quantum for the transition $i_j \to f_j$, $\langle 1|\tilde{r}|0\rangle_j^2 = \hbar/2m_0\omega_j$ is the frequency corrected squared matrix element of the transition $0 \to 1$. Using Eqs. (3) and (4), one obtains

$$Q(E, \varepsilon, y, \vartheta_{10}, \varphi_{10}, \vartheta_{20}, \varphi_{20}) \approx \frac{\theta'}{4\theta}\frac{\cos^2\vartheta_{10}\cos^2\varphi_{10}}{\sinh^2[\pi\omega_1/\alpha u\gamma(\varepsilon, y, \vartheta_{10}, \varphi_{10}, \vartheta_{20}, \varphi_{20})]} \tag{10}$$

$$G(E, \varepsilon, y, \vartheta_{10}, \varphi_{10}, \vartheta_{20}, \varphi_{20}) \approx \cos^2\vartheta_{10}\cos^2\varphi_{10}\cos^2\vartheta_{20}\cos^2\varphi_{20} \times [\gamma(\varepsilon, y, \vartheta_{10}, \varphi_{10}, \vartheta_{20}, \varphi_{20})\alpha u/2]^2 1/\omega_1\omega_2[\xi/\sinh(\xi)]^2$$

$$\xi = \pi(\omega_1 - \omega_2)/\alpha u \tag{11}$$

In Eqs. (10) and (11), $\theta' = 4\pi^2\omega_1^2 m/\alpha^2 k$, $\theta = \hbar\omega_1/k$, and $u = \sqrt{(2E/m)}$. Two different symbols, i.e., ϑ and θ, are being used throughout the paper for the rotation angle and the characteristic vibrational temperature, respectively. The product $u\gamma$ can be interpreted as an effective collision velocity. One can see that at $\varepsilon = y = \vartheta_{i0} = \varphi_{i0} = 0$ one has $\gamma = 1$, $E = E_{\mathrm{tr}}$, and Eqs. (10) and (11) coincide with the one-dimensional probabilities of the single-quantum transitions $0 \to 1$ and $1, 0 \to 0, 1$, predicted by the SSH theory.[24,39] The difference between the present FHO-FR model and the one-dimensional SSH theory result is that Eqs. (4), (10), and (11) incorporate three-dimensional trajectories of rotating molecules as well as the coupling of vibrational states during a collision.

III. Comparison with Trajectory Calculations

To verify the accuracy of the present model, it has to be compared with three-dimensional semiclassical trajectory calculations for the diatom-diatom collisions for the potential energy surface given by Eq. (2). For this purpose we have used the computer codes DIDIAV and DIDIEX developed by Billing.[42,43] Both codes calculate classical translational-rotational collision trajectories. The main difference between the two codes is that DIDIAV uses the FHO formalism,[28–30] modified by Kelley,[31] to evaluate semiclassical vibrational transition probabilities of a frequency corrected harmonic oscillator, whereas in DIDIEX the semiclassical probabilities are evaluated by solving a set of coupled equations for the time-dependent expansion coefficients of the vibrational wave function over a basis of stationary states of the molecules. Although the second approach is certainly more accurate, the calculation time using DIDIEX is about an order of magnitude longer. Both codes give close results (within 10–30%) except for the multiquantum V–T probabilities at high collision energies, for which the DIDIEX predictions are preferred. Calculations were made for collisions of two N2 molecules. The coupling matrix elements $\langle i|\tilde{r}|i \pm 1\rangle$ used by DIDIEX were calculated for the frequency-corrected harmonic oscillator (i.e., with harmonic wave functions but anharmonic energy spectrum), with up to 10 states used for the vibrational wavefunction expansion. The frequency-corrected harmonic oscillator approximation also implies that parameter ω in the FHO-FR model is evaluated as the average vibrational quantum of a transition, i.e., $\omega = |E_i - E_f|/s\hbar$. The N_2 vibrational quantum, the anharmonicity, and the equilibrium atom separation were taken to be $\omega_e = 2359.6$ cm^{-1}, $\omega_e x_e = 14.456$ cm^{-1}, and $r_e = 1.094$ A. The intermolecular repulsive potential parameters used were $A = 1730$ eV and $\alpha = 4.0$ A^{-1} (Ref. 19).

The calculation results are summarized in Figs. 2–7. We emphasize that in the present paper we will always compare the absolute values of the analytic FHO-FR probability and numerical

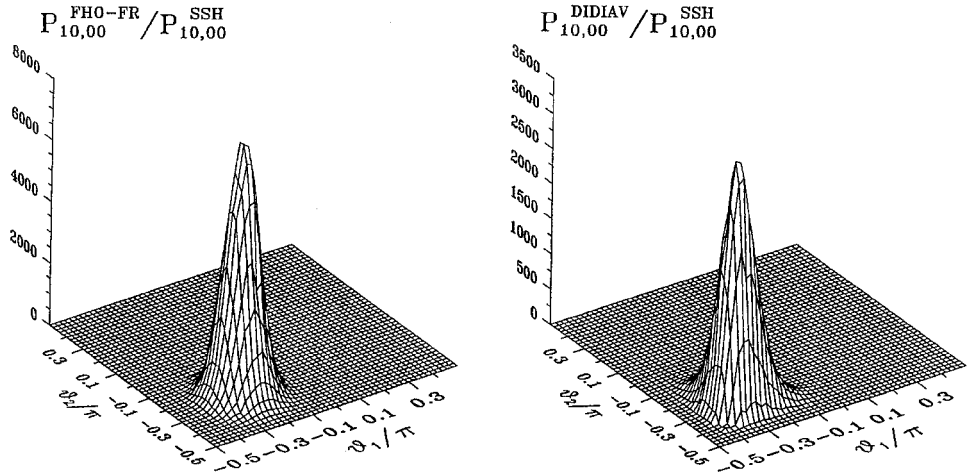

Fig. 2 Comparison of the analytic FHO-FR probability and the numerical DIDIAV probability of the V-T transition $(1,0 \rightarrow 0,0)$ for N_2–N_2 as functions of the rotation angles ϑ_1 and ϑ_2. The total collision energy is $E = 1000\ \mathrm{cm}^{-1}$, $\varepsilon_1 = \varepsilon_2 = \frac{1}{6}$, $b = 0$.

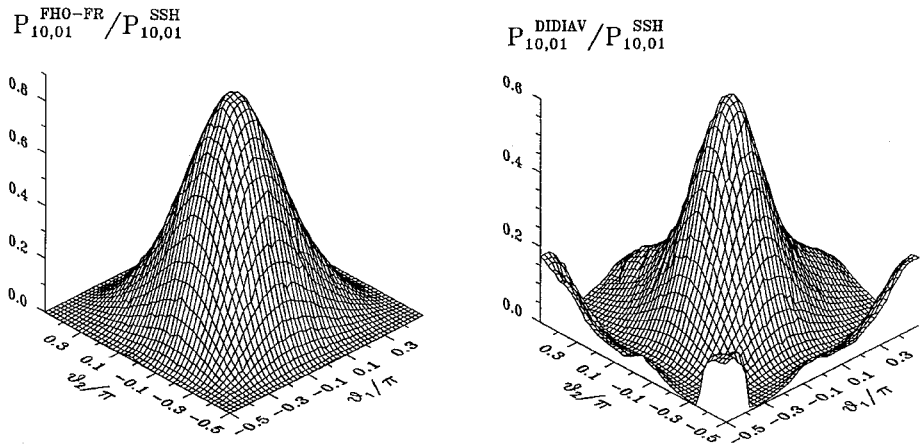

Fig. 3 Comparison of the analytic FHO-FR probability and the numerical DIDIAV probability of the V-V transition $(1,0 \rightarrow 0,1)$ for N_2–N_2 as functions of the rotation angles ϑ_1 and ϑ_2. The total collision energy is $E = 1000\ \mathrm{cm}^{-1}$, $\varepsilon_1 = \varepsilon_2 = \frac{1}{6}$, $b = 0$.

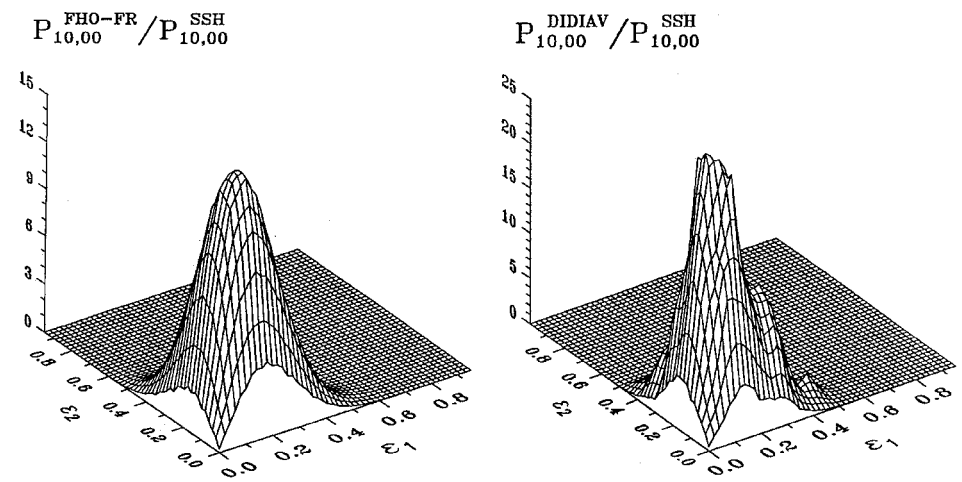

Fig. 4 Comparison of the analytic FHO-FR probability and the numerical DIDIAV probability of the V-T transition $(1,0 \rightarrow 0,0)$ for N_2–N_2 both averaged over the collision angles ϑ_1, ϑ_2, φ_1, and φ_2, as functions of the rotational energies ε_1 and ε_2. The total collision energy is $E = 1000\ \mathrm{cm}^{-1}$, $b = 0$.

probability, respectively, evaluated for two identical potential energy surfaces. We will also use the one-dimensional, collinear-collision SSH probabilities $P^{\mathrm{SSH}}_{10,00}(E) = (\theta'/4\theta)\sinh^{-2}(-\pi\omega/\alpha u)$ and $P^{\mathrm{SSH}}_{10,01}(E) = (\alpha u 2\omega)^2$ only as convenient scale factors. This procedure is more challenging than comparison of the two relative probabilities (i.e., analytic vs numerical), both normalized on their respective values at some reference point, which is commonly used for validation of analytic rate models. For brevity, let us omit the subscript 0 remembering, however, that from now on the angles ϑ_i and φ_i are always evaluated at the maximum interaction point. Figure 2 shows the ratio of the three-dimensional FHO-FR V-T transition probability $P_{10,00}(E, \varepsilon_1, \varepsilon_2, y, \vartheta_1, \vartheta_2, \varphi_1, \varphi_2)$, given by Eqs. (4), (6), and (10), to the SSH probability $P^{\mathrm{SSH}}_{10,00}(E)$, as a function of the rotation angles ϑ_1, ϑ_2. All other collision parameters were held constant at $E = 10^3\ \mathrm{cm}^{-1}$, $\varphi_1 = \varphi_2 = 0$, $\varepsilon_1 = \varepsilon_2 = \frac{1}{6}$, $y = b^2/R_0^2 = 0$. Also shown in Fig. 2 is the ratio of the DIDIAV transition probability,

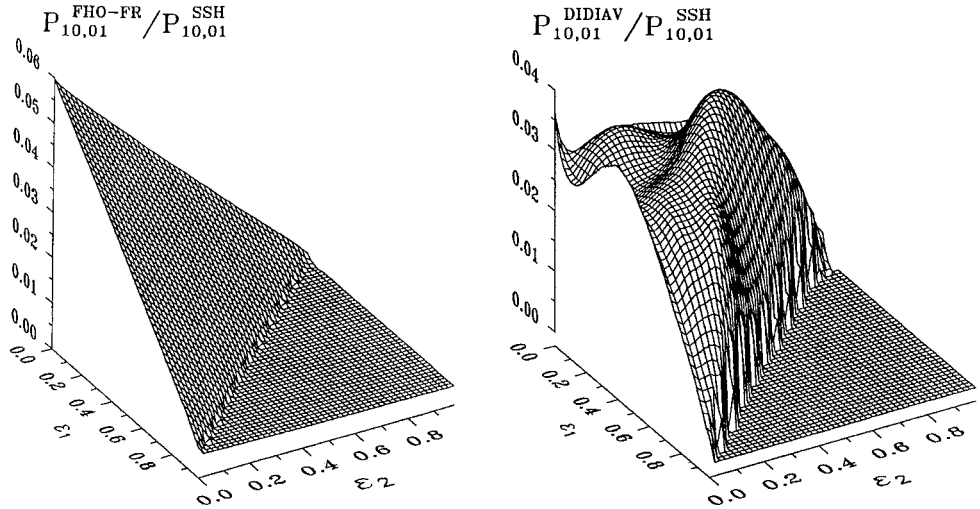

Fig. 5 Comparison of the analytic FHO-FR probability and the numerical DIDIAV probability of the V-V transition $(1, 0 \rightarrow 0, 1)$ for N_2–N_2 both averaged over the collision angles ϑ_1, ϑ_2, φ_1, and φ_2, as functions of the rotational energies ε_1 and ε_2. The total collision energy is $E = 1000\ \text{cm}^{-1}$, $b = 0$.

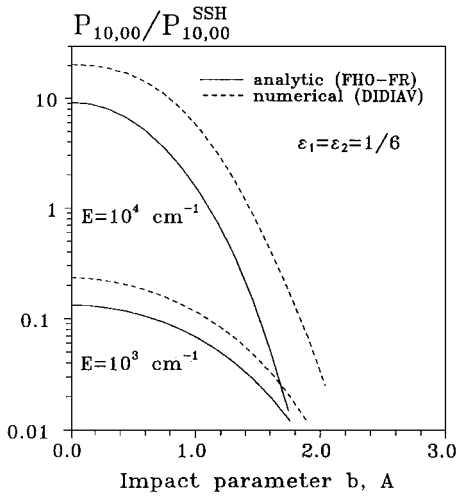

Fig. 6 Comparison of the analytic FHO-FR probaility and the numerical DIDIAV probability of the V-T transition $(1, 0 \rightarrow 0, 0)$ for N_2–N_2, both averaged over the collision angles ϑ_1, ϑ_2, φ_1, and φ_2, as functions of impact parameter b. $\varepsilon_1 = \varepsilon_2 = \frac{1}{6}$.

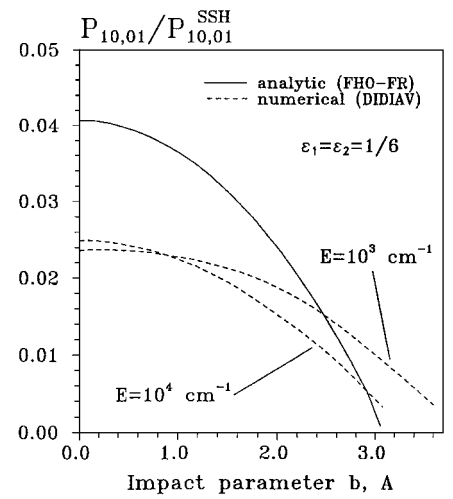

Fig. 7 Comparison of the analytic FHO-FR probability and the numerical DIDIAV probability of the V-V transition $(1, 0 \rightarrow 0, 0)$ for N_2–N_2, both averaged over the collision angles ϑ_1, ϑ_2, φ_1, and φ_2, as functions of impact parameter b. $\varepsilon_1 = \varepsilon_2 = \frac{1}{6}$.

evaluated for the same collision parameters, to the same factor $P^{\text{SSH}}_{10,00}(E)$. One can see that the FHO-FR probability peaks at similar values of the rotation angles as the DIDIAV probability ($\vartheta_1 = \vartheta_2 \cong -0.25\pi$ vs $\vartheta_1 = \vartheta_2 \cong -0.3\pi$). The optimum configuration for the V-T energy transfer is noncollinear. The maximum probability, which exceeds $P^{\text{SSH}}_{10,00}$ by more than three orders of magnitude, is also predicted quite accurately (within a factor of two). Figure 3 shows the ratios of the FHO-FR and DIDIAV V-V probabilities $P_{10,01}$, calculated at the same conditions as in Fig. 2, to the SSH probability $P^{\text{SSH}}_{10,01}(E)$. Both analytic and numerical probabilities are maximum for the collinear configuration ($\vartheta_1 = \vartheta_2 = 0$), and the maximum probability is predicted by the FHO-FR model with accuracy of 20%. From Fig. 3 one can see that the analytic V-V probability is zero for the perpendicular orientation of at least one of the molecules at the point of maximum interaction ($\vartheta_1 = \pm\pi/2$ and/or $\vartheta_2 = \pm\pi/2$), while the numerical probability in these cases can be different from zero. This illustrates that the free rotation approximation, which works well for the V-T processes induced over a small portion of the trajectory near the maximum interaction point, is less accurate for the resonance V-V processes that occur over a much longer portion of the trajectory [compare the integrals in Eqs. (8) and (9)]. This "nonlocal" character of the resonance V-V energy transfer makes it rather sensitive to the change of the orientation angles caused by the forced (i.e., nonfree) molecular rotation during the collision.

Figure 4 plots the ratios of the FHO-FR and DIDIAV V-T probabilities $P_{10,00}(E, \varepsilon_1, \varepsilon_2, y)$, averaged over the orientation and angular momentum angles $\vartheta_1, \vartheta_2, \varphi_1, \varphi_2 \in [-\pi/2, \pi/2]$, to the SSH probability $P^{\text{SSH}}_{10,00}(E)$, as a function of the dimensionless rotational energies $\varepsilon_1 = E_{\text{rot},1}/E$ and $\varepsilon_2 = E_{\text{rot},2}/E$. Once again, both probabilities peak at about the same values of ε_1 and ε_2, $\varepsilon_1 \cong \varepsilon_2 \cong 0.2$, and the maximum value is predicted within about 50% accuracy. Note that 1) the most efficient value of rotational energy is within the limits of applicability of the FHO-FR model $\varepsilon_1 + \varepsilon_2 \lesssim \frac{1}{2}$, given by Eq. (5), and 2) the DIDIAV transition probability sharply drops at $\varepsilon_1 + \varepsilon_2 \rightarrow 1$, as discussed in Sec. II. The last result justifies neglecting rapidly rotating molecule collisions (see Sec. II).

Figure 5 displays the ratios of the FHO-FR and DIDIAV V-V probabilities $P_{10,01}(E, \varepsilon_1, \varepsilon_2, y)$, evaluated at the same conditions as in Fig. 5, to the SSH probability $P^{\text{SSH}}_{10,01}(E)$. One can see that the analytic probability linearly decreases with rotational energy, while the numerical probability at $\varepsilon_1, \varepsilon_2 < \frac{1}{2}$ is weakly dependent on the rotational energy. Again, this difference shows that the free rotation approximation is less accurate for the resonance V-V processes than for the V-T processes. As just discussed, the nonlocal character of the resonance V-V energy transfer makes it sensitive to the change of the angular momentum vectors due to the forced rotation during the collision, which explains poor accuracy of the free rotation approximation in this case.

Figures 6 and 7 show the ratios of the FHO-FR and DIDIAV V-T and V-V probabilities, averaged over the orientation and angular momentum angles $\vartheta_1, \vartheta_2, \varphi_1, \varphi_2 \in [-\pi/2, \pi/2]$ to the SSH probabilities $P^{\mathrm{SSH}}_{10,00}(E)$ and $P^{\mathrm{SSH}}_{10,01}(E)$, respectively, as functions of the impact parameter b. Both figures show the probability ratios calculated at two collision energies $E = 10^3$ and 10^4 cm^{-1} at $\varepsilon_1 = \varepsilon_2 = \frac{1}{6}$. One can see that both V-T and V-V analytic probabilities are within a factor of two of the numerical results, although the impact parameter dependence of the FHO-FR V-T probabilities is in much better agreement with the trajectory calculations. This again shows that the modified wave-number approximation, discussed in Sec. II, works better for the "local" V-T processes than for the nonlocal resonance V-V processes.

The fact that the ratios $P^{\mathrm{FHO\text{-}FR}}_{10}/P^{\mathrm{SSH}}_{10}$ and $P^{\mathrm{DIDIAV}}_{10}/P^{\mathrm{SSH}}_{10}$ both greatly exceed unity at $\vartheta_1, \vartheta_2, \varepsilon_1, \varepsilon_2 \neq 0$ (see Figs. 2 and 4) demonstrates that noncollinear collisions of rotating molecules are much more efficient for V-T energy transfer than head-on collinear collisions of nonrotating molecules considered by the SSH theory. The same effect, caused by the perturbation of the interaction potential near the maximum interaction point by molecular rotation, has been observed in atom-molecule collisions and discussed in Refs. 36 and 37.

Comparison of the two-quantum transition probabilities $P_{20,00}$ and $P_{20,02}$ with the trajectory calculations by DIDIAV demonstrated the same kind of agreement (i.e., between a few tens of percent and a factor of two).

To compare the analytic and the numerical transition probabilities as functions of only the total collision energy E, we numerically averaged the probabilities $P_{\mathrm{VT}}(i_1, 0 \rightarrow f_1, 0, E, \varepsilon_i, y, \vartheta_i, \varphi_i)$, given by Eqs. (4), (6), and (10), and $P_{\mathrm{VV}}(i_1, i_2 \rightarrow f_1, f_2, E, \varepsilon_i, y, \vartheta_i, \varphi_i)$, given by Eqs. (4), (7), and (11), over the values of rotational energy, impact parameter, and orientation angles, using 10^5 points randomly chosen in phase space. The respective numerical transition probabilities in a collision energy range $E = 10^2 - 10^6$ cm^{-1} were obtained by Monte Carlo averaging over 1000 randomly chosen trajectories with the same value of E, which provided 10–20% accuracy. The initial separation between a molecule and an atom was 15 A, and the maximum impact parameter was 2.5 A.

Figure 8 compares the FHO-FR and the DIDIEX V-T probabilities. One can see the remarkable agreement in the entire collision energy range considered, both for single-quantum and multiquantum processes, up to $s = 5$. Figure 9 shows that the agreement is also very good for the V-T probabilities at high vibrational quantum numbers, $i \sim 40$. To illustrate a breakdown of the one-dimensional first-order perturbation theory (SSH theory), Fig. 9 also shows the SSH probability of the vibrational transition $(40, 0 \rightarrow 39, 0)$, which is in complete disagreement with both the three-dimensional model (FHO-FR) and the trajectory calculations. Calculations using DIDIEX are rather time-consuming, especially for multiquantum processes, which require a large number of vibrational states in each molecule for the wave-function expansion. Therefore the rest of calculations has been performed using a simpler code DIDIAV. The difference between the predictions of the two codes typically does not exceed 10–30%, except for the multiquantum quantum processes at high collision energies ($E \geq 10^5$ cm^{-1} for transitions $(i, 0 \rightarrow 0, 0)$ in nitrogen), when the difference increases up to a factor of 2–3. At these conditions the predictions of DIDIEX are considered to be more accurate.

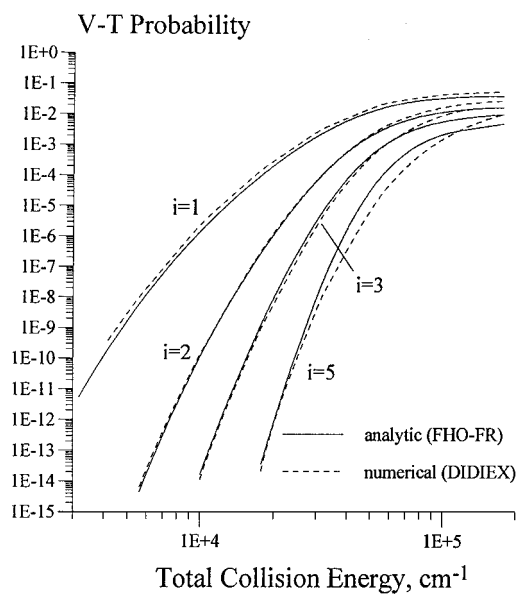

Fig. 8 Comparison of analytic and numerical probabilities of V-T transitions $(i, 0 \rightarrow 0, 0)$ for N_2–N_2.

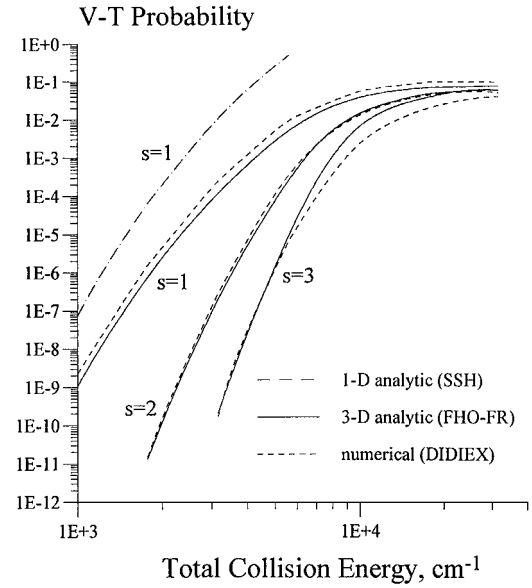

Fig. 9 Comparison of analytic and numerical probabilities of V-T transitions $(i, 0 \rightarrow i - s, 0)$ for N_2–N_2, $i = 40$.

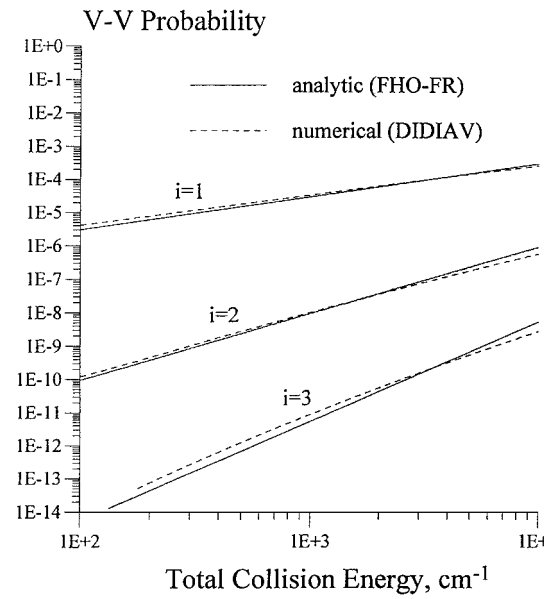

Fig. 10 Comparison of analytic and numerical probabilities of resonance V-V transitions $(i, 0 \rightarrow 0, i)$ for N_2–N_2.

Figures 10–12 compare the FHO-FR and the DIDIAV V-V probabilities. Again, the agreement is quite satisfactory both for the resonance (Figs. 10 and 11) and nonresonance (Fig. 12) single-quantum and multiquantum V-V processes. The SSH probability of the transition $(40, 39 \rightarrow 39, 40)$, shown in Fig. 11, completely disagrees with both three-dimensional models in the entire collision energy range, which again illustrates that one-dimensional perturbation theories are inapplicable for the high vibrational quantum numbers.

The results of the model validation calculations just discussed demonstrate that the analytic FHO-FR formulas given by Eqs. (4),

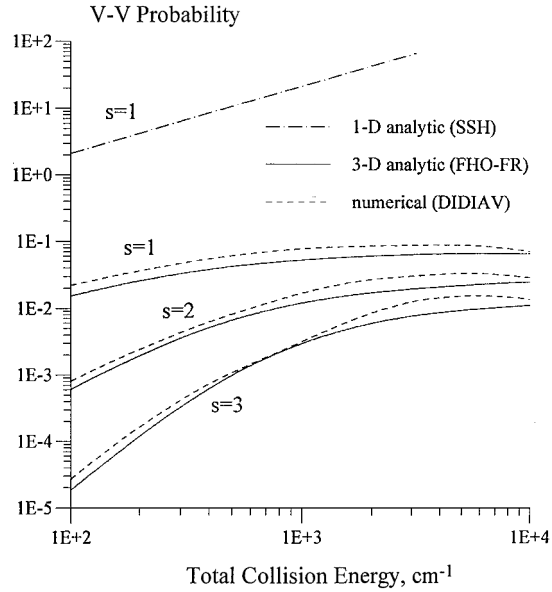

Fig. 11 Comparison of analytic and numerical probabilities of resonance V-V transitions $(i, i-s \rightarrow i-s, i)$ for N_2–N_2 $i = 40$.

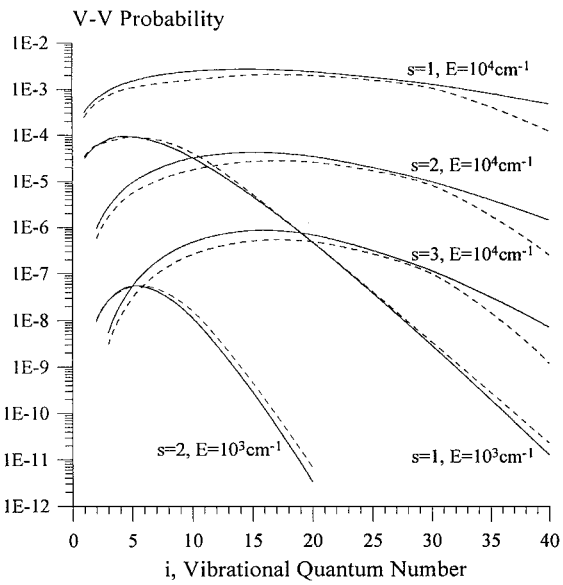

Fig. 12 Comparison of analytic and numerical probabilities of nonresonance V-V transitions $(i, 0 \rightarrow i-s, s)$ for N_2–N_2: ——, analytic (FHO-FR) model; – – –, trajectory calculations by DIDIAV.

(6), (7), (10), and (11) accurately predict the transition probability dependence on all collision parameters such as total collision energy, molecular orientation during the collision, rotational energies, and impact parameter. The model is applicable in a very wide range of collision energies and vibrational quantum numbers, as well as for processes of transfer of many vibrational quanta. Thus, taking into account 1) modulation of the interaction potential by the molecular rotation which is assumed to be free, 2) nonzero impact parameters collisions using the modified wave-number approximation, and 3) many-state coupling using the FHO model, permits capturing the principal mechanism of molecule-to-molecule vibrational energy transfer and gives an accurate three-dimensional analytic rate model.

IV. Averaging the Probabilities and Discussion

To make the FHO-FR model useful for practical calculations, we have to find the transition probabilities as functions of total collision energy E, that is to integrate the probabilities over the angles ϑ_1, ϑ_2, φ_1, φ_2, the rotational energies ε_1 and ε_2, and the impact parameter y. The multidimensional integral is evaluated by steepest descent method, which typically introduces an integration error of about 30–70%. Following the procedure,[37] we first obtain the optimum configuration when the V-T probability at the given total collision energy E reaches maximum:

$$\vartheta_1^* = \vartheta_2^* = -\pi/4, \qquad \varphi_1^* = \varphi_2^* = 0, \qquad \varepsilon_1^* = \varepsilon_2^* = \tfrac{1}{6}$$
$$y^* = 0, \qquad \gamma^* = \sqrt{3/2} \tag{12}$$

The location of the optimum configuration is in excellent agreement with the predictions of the trajectory calculations (see Sec. III, Figs. 2, 4, and 6). The maximum probability for this optimum configuration $P(i_1, 0 \rightarrow f_1, 0)^*$ is given by Eq. (6), where now

$$Q^* = \frac{\theta'}{2\theta} \exp\left(-\frac{2\pi\omega}{\alpha u\sqrt{3/2}} \right) \tag{13}$$

The superscript * will denote the optimum configuration parameters through the remainder of this paper. One can see that zero impact parameter collisions ($y^* = 0$) are most efficient for the vibrational energy transfer. However, the probability reaches maximum for a noncollinear collision ($\vartheta_1^* = \vartheta_2^* = -\pi/4$) of rotating molecules ($\varepsilon_1^* = \varepsilon_2^* = \frac{1}{6}$), when the angular momentum vector is perpendicular to the velocity vector v near the point of maximum interaction ($\varphi_1^* = \varphi_2^* = 0$) (see Fig. 1). Expanding the probability of Eq. (6) in a series near the optimum configuration point (12) and integrating, one obtains

$$P(i_1, 0 \rightarrow f_1, 0, E, Q^* < s\text{th}) \approx \frac{(n_s)^s}{(s!)^2} \left(\frac{3}{2}\right)^4 \left(\frac{\alpha u}{\pi\omega s}\right)^4 (Q^*)^s$$
$$\times \exp\left[-\frac{2n_s}{s+1} Q^* - \frac{n_s^2}{(s+1)^2(s+2)} Q^{*2} \right] \tag{14}$$

where Q^* is given by Eq. (13) and

$$s\text{th} = \frac{(s+1)(s+2)}{2n_s} \left(\sqrt{\frac{3s+2}{s+2}} - 1 \right) \tag{15}$$

At $Q^* \geq s\text{th}$, i.e., at the high collision energies, the procedure for the probability integration becomes more cumbersome because the optimum configuration of collision parameters, such as those given by Eq. (12) is no longer unique (see discussion in Ref. 37).

Repeating this procedure for the V-V processes, we obtain the optimum configuration, which in this case is collinear,

$$\vartheta_1^* = \vartheta_2^* = \varphi_1^* = \varphi_2^* = \varepsilon_1^* = \varepsilon_2^* = y^* = 0, \qquad \gamma^* = 1 \tag{16}$$

Again, the location of this optimum configuration is in excellent agreement with the predictions of the trajectory calculations (see Sec. III, Figs. 3, 5, and 7). The maximum probability for the optimum configuration is given by Eq. (7), where

$$G^* = \left(\frac{\alpha u}{2}\right)^2 \frac{1}{\omega_1\omega_2} \left[\frac{\xi}{\sinh(\xi)} \right]^2, \qquad \xi = \frac{\pi(\omega_1 - \omega_2)}{\alpha u} \tag{17}$$

Expansion the probability of Eq. (7) in a series near the optimum configuration point (16) and integration over the angles, rotational energies, and impact parameters, gives

$$P(i_1, i_2 \rightarrow f_1, f_2, E, G^* < s\text{th})$$
$$= \underbrace{\frac{(1 + 1/2^{s-1})^4}{2^{s+8}(s+1)^2}}_{F(s)} \frac{(n_{s,1})^s (n_{s,2})^s}{(s!)^2} (G^*)^s$$
$$\times \exp\left[-\frac{2n_s}{s+1} G^* - \frac{n_s^2}{(s+1)^2(s+2)} G^{*2} \right] \tag{18}$$

where now

$$s\text{th} = \frac{(s+1)(s+2)}{2n_{s,1}n_{s,2}} \left(\sqrt{\frac{3s+2}{s+2}} - 1 \right) \tag{19}$$

At $s = 1$ and $G^* \ll 1$, Eq. (18) looks almost exactly as the expression for the one-dimensional SSH probability $(1, 0 \rightarrow 0, 1)$ (Ref. 39) except for the factor $F(1) = \frac{1}{128}$. This is the three-dimensional steric factor that describes the V-V probability reduction caused by noncollinear orientation, molecular rotation, and nonzero impact parameter collisions. Again, at the high collision energies, such as $G^* \geq s^{\text{th}}$, nonuniqueness of the optimum configuration substantially complicates the analysis. The complete closed-form expressions for the V-T and V-V probabilities that span both low and high collision energies, such as obtained for atom-molecule collisions in Ref. 37, will be given in our next publication.

Thermally averaged relaxation rate coefficients can be determined by averaging of the transition cross sections over the Boltzmann distribution[42]:

$$k(i_1, i_2 \rightarrow f_1, f_2, T) = \langle u \rangle \int_0^\infty \sigma(\bar{E}) \exp\left(-\frac{\bar{E}}{T}\right) \mathrm{d}\left(\frac{\bar{E}}{T}\right)$$

$$= \pi R_0^2 \langle u \rangle \int_0^\infty \left(\frac{\bar{E}}{T}\right)^3 P(\bar{E}) \exp\left(-\frac{\bar{E}}{T}\right) \mathrm{d}\left(\frac{\bar{E}}{T}\right) \qquad (20)$$

In Eq. (20), $\langle u \rangle = (8kT/\pi m)^{1/2}$, $\bar{E} = E + \Delta E/2 + (\Delta E)^2/16E$ is the symmetrized collision energy,[42] ΔE is vibrational energy defect, $\sigma(\bar{E})$ is the cross section, and $P(\bar{E})$ is the transition probability. The factor $\pi R_0^2 \cdot (\bar{E}/T)^3$ in the expression for the cross section appears as a result of integration over the values of orbital kinetic energy (or orbital angular momentum) and two rotational energies (or rotational angular momenta).[42] The maximum interaction distance R_0 is found as $U(R_0) = kT$, $R_0 \cong 2.5A$ at $T \sim 10^4$ K. Then the effective cross section for elastic collisions is $\langle\langle \sigma_{\text{el}} \rangle\rangle = k_{\text{el}}(T)/\langle u \rangle = 3\pi R_0^2 \approx 60\, A^2$, and the gas kinetic collision frequency is $Z = 3\pi R_0^2 \langle u \rangle$.

Evaluation of the integral in Eq. (20) using the V-T probability (14) yields

$$k(i_1, 0 \rightarrow f_1, 0, T) = Z \frac{9}{2} \sqrt{\frac{2\pi}{3}} \frac{(n_s)^s}{(s!)^2} \left(\frac{\theta'}{2\theta}\right)^s \left(\frac{Ts^2}{\theta'}\right)^{\frac{1}{6}}$$

$$\times \exp\left\{-\frac{3}{2}\left[\frac{\theta' s^2}{(3/2)T}\right]^{\frac{1}{3}}\right\}$$

$$\times \exp\left(-\frac{2n_s}{s+1} \exp\left\{-\frac{3}{2}\left[\frac{\theta'}{\frac{3}{2}sT}\right]^{\frac{1}{3}}\right\}\right.$$

$$\left. - \frac{n_s^2}{(s+1)^2(s+2)} \exp\left\{-3\left[\frac{\theta'}{\frac{3}{2}sT}\right]^{\frac{1}{3}}\right\}\right)$$

$$\times \exp\left(\frac{\theta s}{2T}\left\{1 - \frac{\theta}{4T}\left[\frac{\frac{3}{2}T}{\theta' s^2}\right]^{\frac{1}{3}}\right\}\right) \qquad (21)$$

The last exponential factor in Eq. (21) originates from the symmetrization of collision energy in Eq. (20). Following the procedure suggested in Ref. 42, we evaluate the rates of exothermic processes. The endothermic rates can be found simply as $k_{\text{endo}} = k_{\text{exo}} \cdot \exp(-\theta s/T)$. Equation (21) is valid only if $T \leq T\text{th}$, where $T\text{th}$ is the threshold temperature that corresponds to the "switching" from the unique to the multiple optimum configuration regime (see Ref. 37),

$$T\text{th} = \frac{2\theta'}{33\, \ell n^2[\theta'/3s\,\text{th}\,\theta]} \qquad (22)$$

The values of the threshold temperature for N_2–N_2 collisions, given by Eq. (22), change from $T\text{th} = 11{,}000$ K for the transition $1 \rightarrow 0$–$T\text{th} = 1300$ K for the transition $40 \rightarrow 39$. More elaborate integration is needed to obtain the closed-form analytic V-T rates at higher temperatures.

Integration of Eq. (20) using the V-V probability of Eq. (18) at $\xi = 0$ (for the resonance V-V processes) yields

$$k(i_1, i_2 \rightarrow i_2, i_1, T) = Z \underbrace{\frac{(1 + 1/2^{s-1})^4}{2^{s+8}(s+1)^2} \frac{(s+3)!}{3!}}_{F(s)}$$

$$\times \frac{(n_{s,1})^s (n_{s,2})^s}{(s!)^2} \left(\frac{\alpha^2 kT}{2m\omega^2}\right)^s 1 \Big/ \left(1 + \frac{2n_{s,1}n_{s,2}}{s+1} F(s) \frac{\alpha^2 kT}{2m\omega^2}\right)^{s+4} \qquad (23)$$

One can see that the thermally averaged three-dimensional steric factor for single-quantum V-V exchange in Eq. (23), $F(1) = \frac{1}{32}$, is different from the value obtained by the modified SSH theory, $\frac{1}{9}$ (Ref. 24), and changes with the number of transmitted quanta s. Integration at $\xi \neq 0$ becomes less straightforward and requires additional analysis, which we intend to complete in our next publication.

Equation (23) is valid if $T \leq T\text{th}$, where $T\text{th}$ is given by

$$T\text{th} = (2m\omega^2/\alpha^2 k)s\text{th} \qquad (24)$$

For N_2–N_2 collisions, $T\text{th} = 4000$ K for the transition $10, 9 \rightarrow 9, 10$ but drops to only $T\text{th} = 250$ K for the transition $40, 39 \rightarrow 39, 40$. Again, more elaborate integration is needed to obtain the closed-form analytic V-V rates at higher temperatures.

Although the complete analytic FHO-FR V-T and V-V rate expressions are not yet available, we compared the rates coefficients obtained by numerical integration of the analytic FHO-FR V-T probabilities given by Eqs. (6),(10), and (20) and V-V probabilities given by Eqs. (7),(11), and (20) over all collision parameters, with trajectory calculations for N_2–N_2. Figures 13 and 14 show that the results are in remarkably good agreement in the temperature range of $200 \leq T \leq 10{,}000$ K and vibrational quantum number range $0 \leq i \leq 40$. Although multiquantum FHO-FR rate coefficients are not shown, comparison of the probabilities in Figs. 8–12 leaves no doubt that the agreement is equally good.

Finally, the FHO-FR model predictions for O_2–O_2 relaxation rates have been compared with 1) experimental data,[6–8] 2) three-dimensional semiclassical calculations by DIDIAV using the potential energy surface,[20] which takes into account the long-range dispersion and quadrupole-quadrupole interaction terms, and 3) three-dimensional quantum calculations using ab initio potential energy surface,[13] rather than the simplified atom-to-atom potential.[20] Analytic FHO-FR relaxation rates have been evaluated using Eq. (3) with $\alpha = 4.0$ A^{-1}, which has been determined in Ref. 20 from the best fit of the short-range potential energy surface to ab initio data. The results, shown in Fig. 15, again demonstrate good agreement between experimental data, analytic model, and three-dimensional calculations.

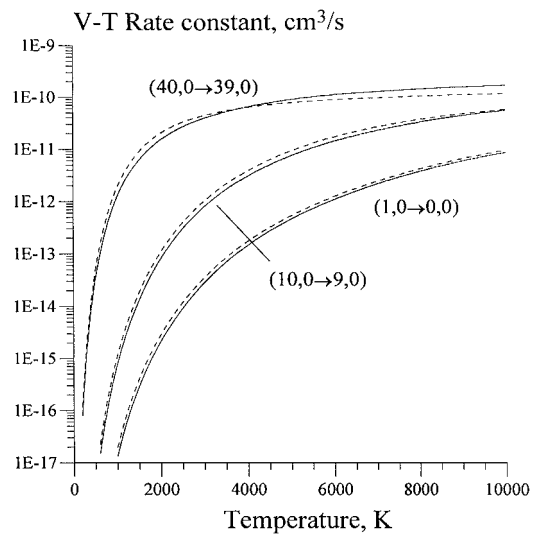

Fig. 13 Comparison of the analytic (——) and numerical (– – –) rates of V-T transitions for N_2–N_2.

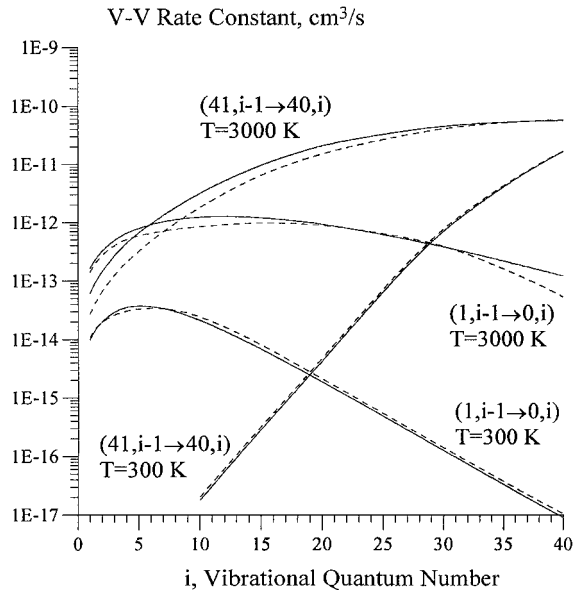

Fig. 14 Comparison of the analytic (——) and numerical (– – –) rates of V-V transitions $(1, i-1 \rightarrow 0, i)$ and $(41, i-1 \rightarrow 40, i)$ for N_2–N_2.

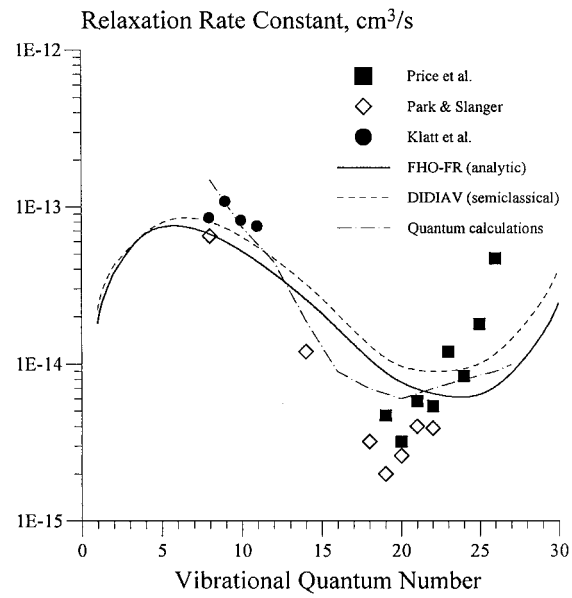

Fig. 15 Comparison of analytic (——), semiclassical (– – –), and quantum (–·–) calculations and experimental relaxation rates in O_2 at room temperature.

V. Summary

Analysis of classical trajectories of free-rotating symmetric diatomic molecules acted upon by a repulsive potential allow extending a three-dimensional semiclassical nonperturbative analytic model of vibrational energy transfer (FHO-FR model) to molecule–molecule collisions. The model takes into account the following coupled effects: 1) interaction potential modulation by free rotation of arbitrarily oriented molecules during a collision, 2) reduction of the effective collision velocity in nonzero impact parameter collisions of rotating molecules, and 3) multistate coupling in a collision.

The FHO-FR model predictions have been compared with close-coupled semiclassical trajectory calculations using the same potential energy surface. The comparison demonstrates not only very good agreement between the analytic and numerical probabilities across a wide range of collision energies, but also shows that the analytic model correctly reproduces the probability dependence on other collision parameters such as rotation angles, angular momentum angles, rotational energies, and impact parameter. The model equally well predicts the cross sections of single-quantum and multiquantum V-T and V-V transitions and is applicable up to very high collision energies and quantum numbers. The resultant analytic expressions for the probabilities do not contain any arbitrary adjustable parameters commonly referred to as steric factors. The results obtained in the present paper can be used for calculations of the state-specific V-T and V-V relaxation rates in collisions of symmetric or nearly symmetric molecules such as N_2–N_2, O_2–O_2, and N_2–O_2. Thus, the present paper essentially completes development of the analytic rate database for vibrational energy transfer among air species, increasing the range of applicability of the FHO-FR model. (Previous results[37] are applicable for N_2–Ar, O_2–Ar, N_2–He, and O_2–He V-T relaxation.) It remains an open question, however, whether the approach used here is applicable for calculations of vibrational energy transfer rates induced by the long-range multipole-multipole interaction, such as occurs in CO–CO and CO–N_2 collisions.

The FHO-FR model provides new insight into kinetics of vibrational energy transfer and provides analytic expressions for state-specific transition probabilities and rate coefficients, applicable in the wide range of collision energies and temperatures that can be easily incorporated into existing nonequilibrium flow codes. Closed-form analytic expressions for the V-T and V-V rates valid in a wide range of collision energies will be completed and published in the near future.

Acknowledgments

This work was supported by the Air Force Office of Scientific Research Space Propulsion and Power Program, Grant F49620-96-1-0184. The authors would like to express their sincere gratitude to J. Daniel Kelley and Sergey O. Macheret for valuable recommendations and numerous useful discussions.

References

[1]Gordiets, B. F., Osipov, V. A., and Shelepin, L. A., *Kinetic Processes in Gases and Molecular Lasers*, Gordon and Breach, London, 1988, Chaps. 3 and 4.

[2]Cacciatore, M., Capitelli, M., DeBenedictis, S., Dilonardo, M., and Gorse, C., "Vibrational Kinetics, Dissociation and Ionization of Diatomic Molecules under Nonequilibrium Conditions," *Nonequilibrium Vibrational Kinetics*, Springer-Verlag, Berlin, 1986, Chap. 2, pp. 5–46.

[3]Park, C., *Nonequilibrium Hypersonic Aerodynamics*, Wiley, New York, 1990, Chap. 3.

[4]Lee, W., Adamovich, I. V., and Lempert, W. R., "Optical Pumping Studies of Vibrational Energy Transfer in High-Pressure Diatomic Gases," *Journal of Chemical Physics*, Vol. 114, No. 13, 2001, pp. 1178–1186.

[5]Yang, X., Kim, E. H., and Wodtke, A. M., "Vibrational Energy Transfer of Very Highly Vibrationally Excited NO," *Journal of Chemical Physics*, Vol. 96, No. 7, 1992, pp. 5111–5122.

[6]Price, J. M., Mack, J. A., Rogaski, C. A., and Wodtke, A. M., "Vibrational-State-Specific Self-Relaxation Rate Constant Measurements of Highly Excited O_2 ($v = 19$–28)," *Chemical Physics*, Vol. 175, No. 1, 1993, pp. 83–98.

[7]Park, H., and Slanger, T. G., "O (X, $v = 8$–22) 300 K Quenching Rate Coefficients for O_2 and N_2, and O_2(X) Vibrational Distribution from 248 nm O3 Photo-Dissociation," *Journal of Chemical Physics*, Vol. 100, No. 1, 1994, pp. 287–300.

[8]Klatt, M., Smith, I. W. M., Tuckett, R. P., and Ward, G. N., "State-Specific Rate Constants for the Relaxation of $O_2(X^3 \sum_g^-)$ from Vibrational Levels $v = 8$ to 11 by Collisions with NO and O," *Chemical Physics Letters*, Vol. 224, Nos. 3, and 4, 1994, pp. 253–257.

[9]Deleon, R., and Rich, J. W., "Vibrational Energy Exchange Rates in Carbon Monoxide," *Chemical Physics*, Vol. 107, No. 2, 1986, pp. 283–292.

[10]Secrest, D., and Johnson, B. R., "Exact Quantum Mechanical Calculations of a Collinear Collision of a Particle with a Harmonic Oscillator," *Journal of Chemical Physics*, Vol. 45, No. 12, 1966, pp. 4556–4570.

[11]Chapuisat, X., Bergeron, G., and Launay, J.-M., "A Quantum-Mechanical Collinear Model Study of the Collision N2–O2," *Chemical Physics*, Vol. 20, No. 2, 1977, pp. 285–298.

[12]Chapuisat, X., and Bergeron, G., "Anharmonicity Effects in the Collinear Collision of Two Diatomic Molecules," *Chemical Physics*, Vol. 36, No. 3, 1979, pp. 397–405.

[13]Hernandez, R., Toumi, R., and Clary, D. C., "State-Selected Vibrational Relaxation Rates for Highly Vibrationally Excited Oxygen Molecules," *Journal of Chemical Physics*, Vol. 102, No. 24, 1995, pp. 9544–9558.

[14]Kuksenko, B. V., and Losev, S. A., "On the Theory of Vibrational Relaxation of Diatomic Molecules," *High Temperature*, Vol. 6, No. 5, 1968, pp. 794–799.

[15]Lagana, A., Garcia, E., and Ciccarelli, L., "Deactivation of Vibrationally Excited Nitrogen Molecules by Collision with Nitrogen Atoms," *Journal of Physical Chemistry*, Vol. 91, No. 2, 1987, pp. 312–314.

[16]Lagana, A., and Garcia, E., "Temperature Dependence of $N + N_2$ Rate Coefficients," *Journal of Physical Chemistry*, Vol. 98, No. 2, 1994, pp. 502–507.

[17]Billing, G. D., "Vibration-Vibration and Vibration-Translation Energy Transfer, Including Multiquantum Transitions in Atom-Diatom and Diatom-Diatom Collisions," *Nonequilibrium Vibrational Kinetics*, Springer-Verlag, Berlin, 1986, Chap. 4, pp. 85–111.

[18]Kolesnick, R. E., and Billing, G. D., "Rate Constants for Vibrational Transitions in Hydrogen and Isotopes," *Chemical Physics*, Vol. 170, No. 1, 1993, pp. 201–207.

[19]Billing, G. D., and Fisher, E. R., "VV and VT Rate Coefficients in N_2 by a Quantum-Classical Model," *Chemical Physics*, Vol. 43, No. 3, 1979, pp. 395–401.

[20]Billing, G. D., and Kolesnick, R. E., "Vibrational Relaxation of Oxygen. State to State Rate Constants," *Chemical Physics Letters*, Vol. 200, No. 4, 1992, pp. 382–386.

[21]Cacciatore, M., and Billing, G. D., "Semiclassical Calculations of VV and VT Rate Coefficients in CO," *Chemical Physics*, Vol. 58, No. 3, 1981, pp. 395–407.

[22]Billing, G. D., "VV and VT Rates in N_2–O_2 Collisions," *Chemical Physics*, Vol. 179, No. 3, 1994, pp. 463–467.

[23]Cacciatore, M., Capitelli, M., and Billing, G. D., "Theoretical Semiclassical Investigation of the Vibrational Relaxation of CO Colliding with $^{14}N_2$," *Chemical Physics*, Vol. 89, No. 1, 1984, pp. 17–31.

[24]Herzfeld, K. F., and Litovitz, T. A., *Absorption and Dispersion of Ultrasonic Waves*, Academic Press, New York, 1959, Chap. 3.

[25]Rapp, D., and Sharp, T. E., "Vibrational Energy Transfer in Molecular Collisions Involving Large Transition Probabilities," *Journal of Chemical Physics*, Vol. 38, No. 11, 1963, pp. 2641–2648.

[26]Rapp, D., and Englander-Golden, P., "Resonant and Near-Resonant Vibrational-Vibrational Energy Transfer Between Molecules in Collisions," *Journal of Chemical Physics*, Vol. 40, No. 2, 1964, pp. 573–575; Rapp, D., and Englander-Golden, P., "Erratum: Resonant and Near-Resonant Vibrational-Vibrational Energy Transfer Between Molecules in Collisions," *Journal of Chemical Physics*, Vol. 40, No. 10, 1964, pp. 3120, 3121; Rapp, D., "Interchange of Vibrational Energy Between Molecules in Collisions," *Journal of Chemical Physics*, Vol. 43, No. 1, 1965, pp. 316, 317.

[27]Sharma, R. D., and Brau, C. A., "Energy Transfer in Near-Resonant Molecular Collisions due to Long-Range Forces with Application to Transfer of Vibrational Energy from 3 Mode of CO_2 to N_2," *Journal of Chemical Physics*, Vol. 50, No. 2, 1969, pp. 924–930.

[28]Kerner, E. H., "Note of the Forced and Damped Oscillations in Quantum Mechanics," *Canadian Journal of Physics*, Vol. 36, No.3, 1958, pp. 371–377.

[29]Treanor, C. E., "Vibrational Energy Transfer in High Energy Collisions," *Journal of Chemical Physics*, Vol. 43, No. 2, 1965, pp. 532–538.

[30]Zelechow, A., Rapp, D., and Sharp, T. E., "Vibrational-Vibrational-Translational Energy Transfer Between Two Diatomic Molecules," *Journal of Chemical Physics*, Vol. 49, No. 1, 1968, pp. 286–299.

[31]Kelley, J. D., "Vibrational Energy Transfer Processes in Collision Between Diatomic Molecules," *Journal of Chemical Physics*, Vol. 56, No. 12, 1972, pp. 6108–6117.

[32]Shin, H. K., "Vibrational Energy Transfer," *Dynamics of Molecular Collisions*, Plenum, New York, 1976, Pt. A, Chap. 4, pp. 131–210.

[33]Schwartz, R. N., and Herzfeld, K. F., "Vibrational Relaxation in Gases (Three-Dimensional Treatment)," *Journal of Chemical Physics*, Vol. 22, No. 2, 1954, pp. 767–773.

[34]Takayanagi, K., "Vibrational and Rotational Transitions in Molecular Collisions," *Supplement to the Progress of Theoretical Physics*, No. 25, 1963, pp. 1–98.

[35]Mies, F. H., and Shuler, K., "Quantum-Mechanical Calculation of Harmonic Oscillator Transition Probabilities. II. Three-Dimensional Impulsive Collisions," *Journal of Chemical Physics*, Vol. 37, No. 1, 1962, pp. 177–181.

[36]Adamovich, I. V., and Rich, J. W., "Three-Dimensional Nonperturbative Analytic Model of Vibrational Energy Transfer in Atom–Molecule Collisions," *Journal of Chemical Physics*, Vol. 109, No. 18, 1998, pp. 7711–7724.

[37]Adamovich, I. V., and Rich, J. W., "Three-Dimensional Nonperturbative Analytic Model of Vibrational Energy Transfer in Atom-Molecule Collisions," *Journal of Chemical Physics*, Vol. 109, No. 18, 1998, pp. 7711–7724.

[38]Nikitin, E. E., and Osipov, A. I., "Vibrational Relaxation in Gases," *Kinetics and Catalysis*, Vol. 4, VINITI, All-Union Inst. of Scientific and Technical Information, Moscow, 1977, Chap. 2.

[39]Rapp, D., and Kassal, T., "The Theory of Vibrational Energy Transfer Between Simple Molecules in Nonreactive Collisions," *Chemical Reviews*, Vol. 69, No. 1, 1969, pp. 61–102.

[40]Adamovich, I. V., Macheret, S. O., Rich, J. W., and Treanor, C. E., "Vibrational Relaxation and Dissociation Behind Shock Waves Part 1: Kinetic Rate Models," *AIAA Journal*, Vol. 33, No. 6, 1995, pp. 1064–1069.

[41]Adamovich, I. V., Macheret, S. O., Rich, J. W., and Treanor, C. E., "Vibrational Energy Transfer Rates Using a Forced Harmonic Oscillator Model," *Journal of Thermophysics and Heat Transfer*, Vol. 12, No. 1, 1998, pp. 57–65.

[42]Billing, G. D., "Rate Constants and Cross Sections for Vibrational Transitions in Atom-Diatom and Diatom-Diatom Collisions," *Computer Physics Communications*, Vol. 32, No. 1, 1984, pp. 45–62.

[43]Billing, G. D., "Rate Constants for Vibrational Transitions in Diatom–Diatom Collisions," *Computer Physics Communications*, Vol. 44, No. 2, 1987, pp. 121–136.

M. Sichel
Associate Editor